Supplementary Material

for

Thermo-Mechanical Properties of Mixed-Matrix Membranes Encompassing Zeolitic Imidazolate Framework and Polyvinylidene-difluoride: ZIF-90/PVDF Nanocomposites

Irina S. Flyagina, E.M. Mahdi, Kirill Titov, and Jin-Chong Tan[*]

Multifunctional Materials & Composites (MMC) Laboratory,
Department of Engineering Science, University of Oxford, Parks Road,
Oxford OX1 3PJ, United Kingdom

[*]jin-chong.tan@eng.ox.ac.uk

Table of Contents

I. Rheology

The measurements were performed on Anton Parr Rheometer Physica MCR301 using a CP25-2 cone with 1.995° angle, 24.946 mm diameter and 51 μm truncation. Flow curves were obtained in a rotation mode, and amplitude sweep and frequency sweep curves were obtained in an oscillation mode. In the flow curve tests, dynamic viscosity was measured while the cone rotation rate varied typically from 0.1 to 3000 s^{-1}. In the amplitude sweep measurements, the storage *G'* and loss *G''* moduli of the viscoelastic liquids (MMM dispersions) were measured with the shear strain increasing from 0.01 to 100%. In the frequency sweep tests, the amplitude of the cone was set to 5%, as this value was found to be the maximum at which *G'* and *G''* do not decline in the amplitude sweep tests; *G'* and *G''* were measured as a function of the angular frequency of the cone, which ranged typically from 0.1 to 400 rad s^{-1}. The number of runs for each liquid sample varied between three and six.

Fig. S1 presents the rheology of 15.5 wt.% PVDF solution in DMF. Viscosity of the solution (Fig. S1 a) decreases slightly from ~1 Pa·s at a rotation rate of 500 s^{-1} to 0.6 Pa·s at higher rotation rates. The amplitude sweep curves (Fig. S1 b) show that the rheological properties of the solution change with time, namely, the liquid becomes a gel. At the first measurement (run 1), the liquid-like structure of the sample is evidenced by the loss modulus *G''* exceeding the storage modulus *G'* over the whole range of the shear strain. However, *G'* increased in every next run and approached the values of *G''*, while the latter was relatively stable and remained in a narrow range of 20-30 Pa. In the last two runs (5 and 6), *G'* exceeded *G''* at low shear strains, and this is an indication of the solution-to-gel transition. The frequency sweep curves (Fig. S1 c) reveal information about links between macromolecules and network structure of a viscoelastic liquid, showing that the PVDF solution is a soft gel. The cross-over of the *G'* and *G''* curves, i.e. the transition from *G'* > *G''* to *G''* > *G'*, indicates a transition from the soft gel structure to a viscoelastic liquid with long macromolecules.

Fig. S2 illustrates the rheology of the 5 wt.% ZIF-90/PVDF dispersion in DMF. Dynamic viscosity of the dispersion (Fig. S2 a) remains relatively stable over the wide range of rotation rates, decreasing gradually from 1 Pa·s at 1000 s^{-1} to 0.6 Pa·s at 3000 s^{-1}. These values of the viscosity are similar to those measured for the neat 15.5 wt.% PVDF solution. The amplitude sweep curves (Fig. S2 b) show that the dispersion transits gradually from liquid state to a gel, since the measured storage modulus G' gradually increases and surpasses the loss modulus *G''*. The frequency sweep curves (Fig. S2 c) have a shape characteristic for a dispersion with weak structure, featuring the cross-over of *G'* and *G''*, i.e. at higher strain rates the structure is broken and the dispersion demonstrates a liquid-like behaviour.

Figure S3 reports the rheology of the 10 wt.% ZIF-90/PVDF dispersion in DMF. Dynamic viscosity (Fig. S3 a) is relatively stable and ranges between 0.6 and 0.4 Pa·s over a wide range of rotation rates. Similar to the neat PVDF solution and the 5 wt.% ZIF-90/PVDF dispersion, the amplitude sweep curves of the 10 wt.% ZIF-90/PVDF dispersion (Fig. S3 b, c) demonstrate that its weak structure transits gradually to a liquid-like state. Thus, it is reasonable to conclude that the rheological properties of the MMM dispersions are similar to and are determined by those of the neat PVDF solution.

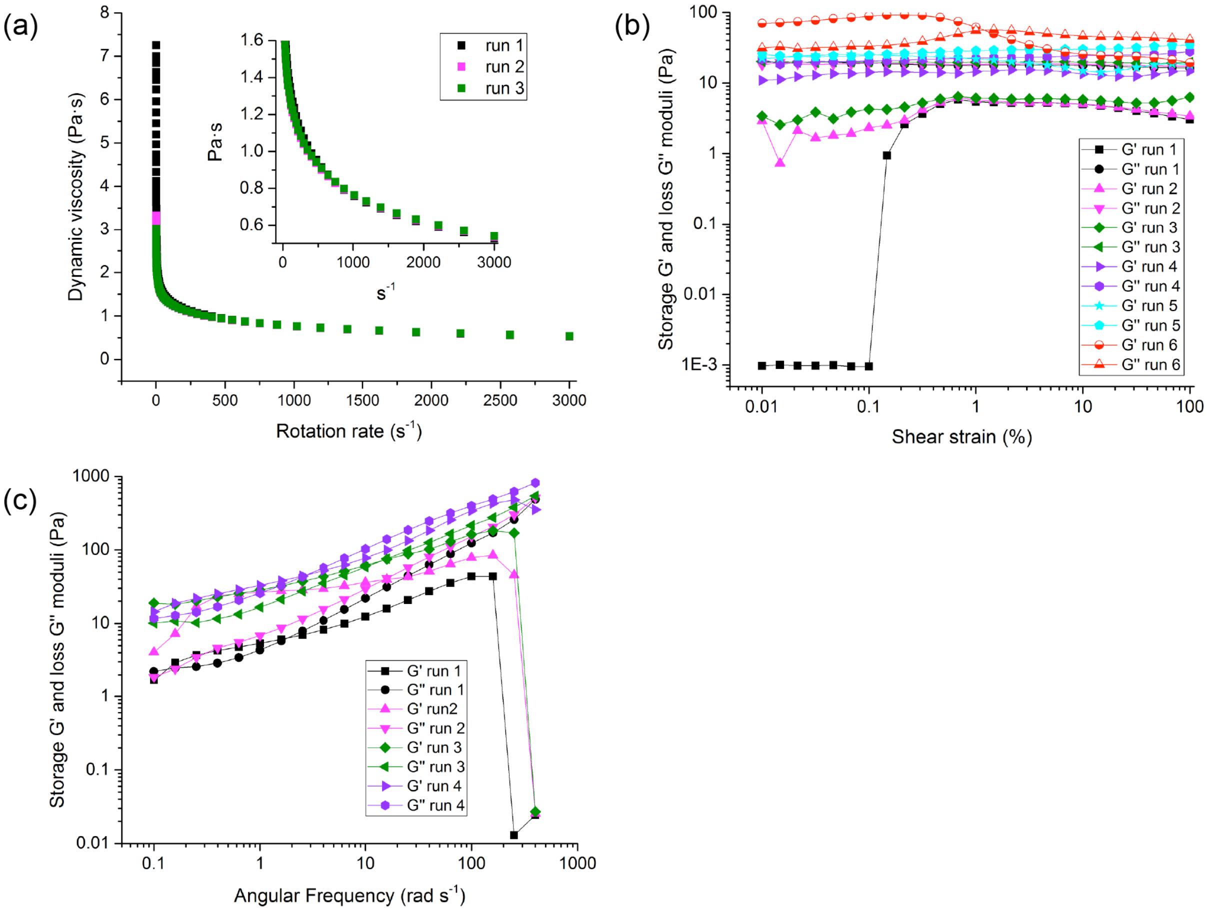

Fig. S1. Rheology of the neat PVDF solution in DMF: a) dynamic viscosity, b) amplitude sweep, and c) frequency sweep curves. The storage *G'* and loss *G''* moduli measured in each run are represented in the same colour for convenience of reading.

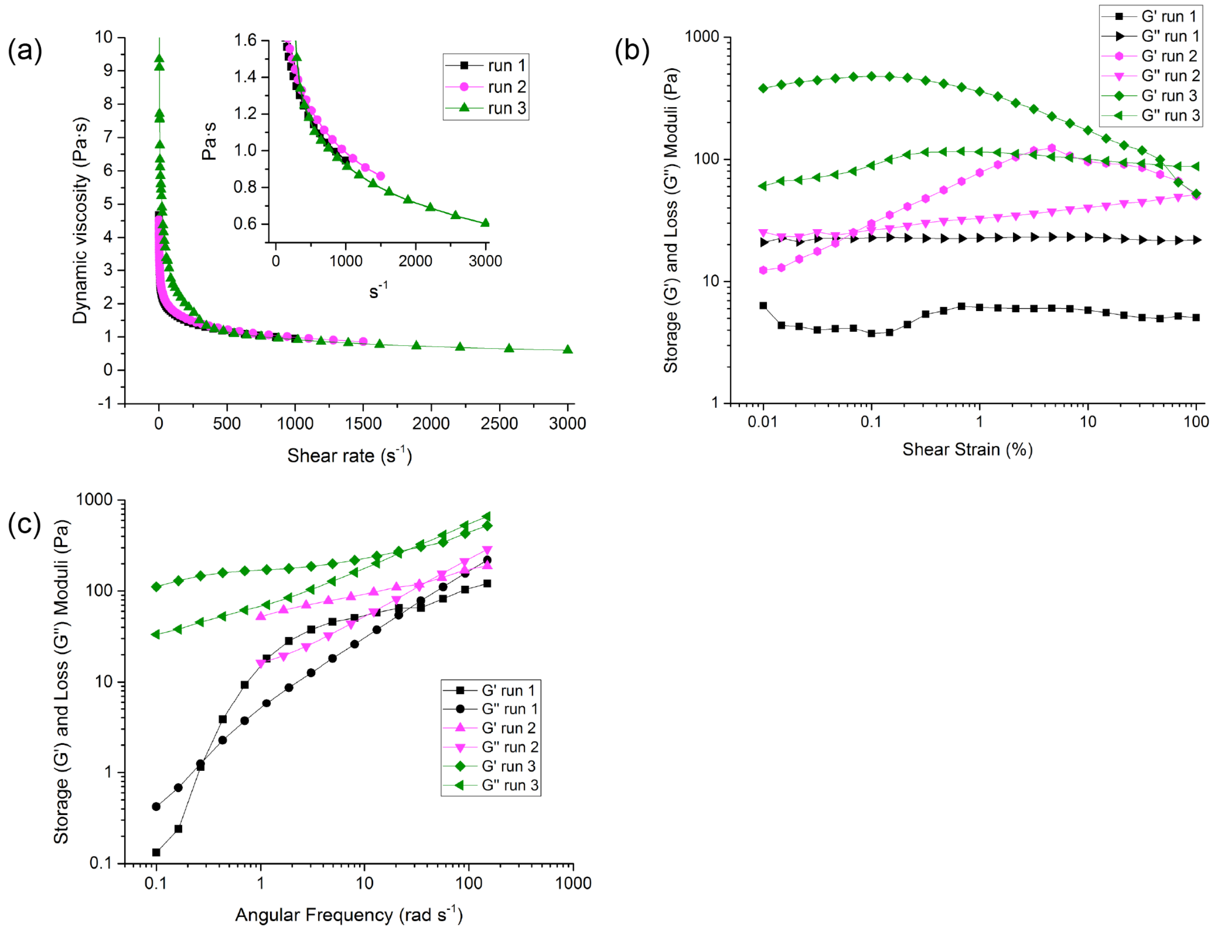

Fig. S2. Rheology of the 5 wt.% ZIF-90/PVDF dispersion in DMF: a) dynamic viscosity, b) amplitude sweep, and c) frequency sweep curves. The storage *G'* and loss *G''* moduli measured in each run are represented in the same colour for convenience of reading.

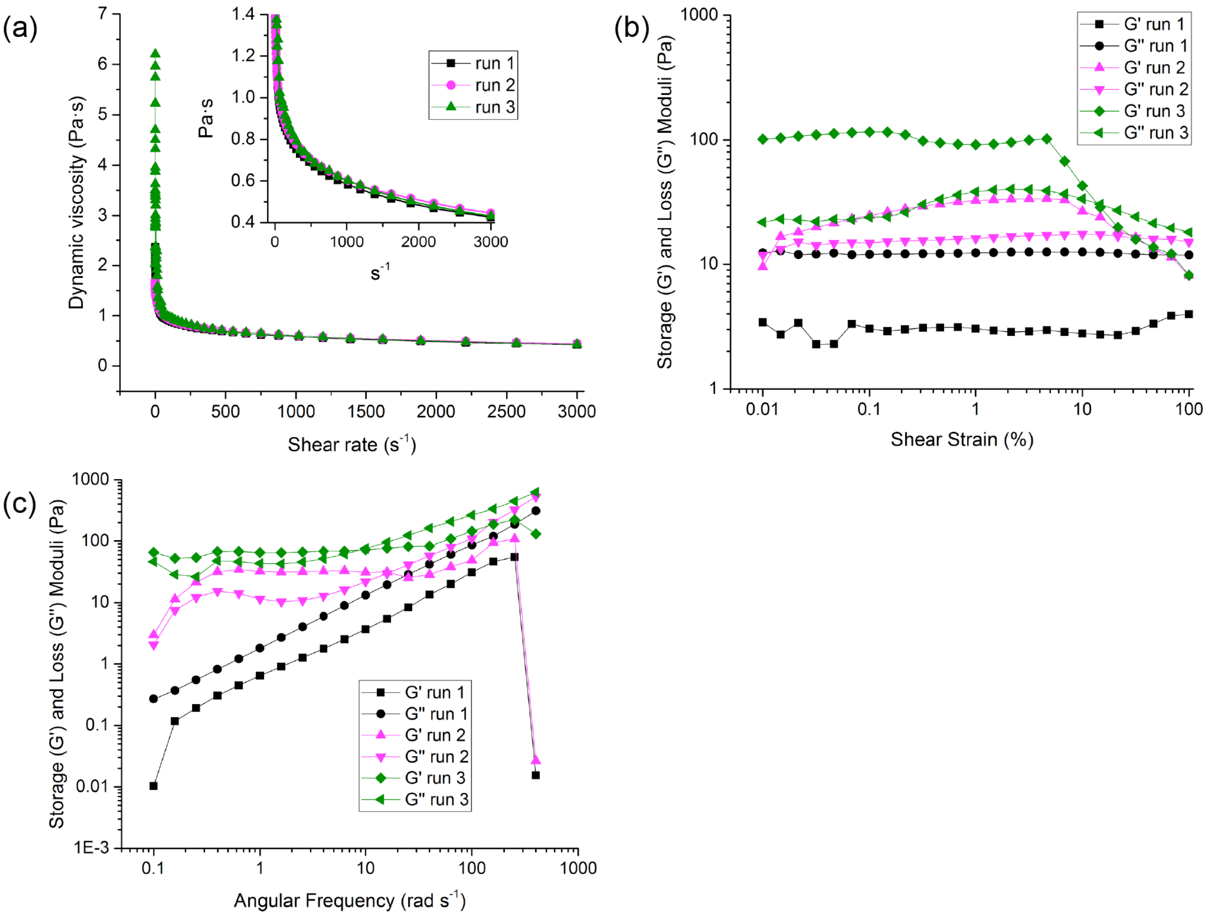

Fig. S3. Rheology of the 10 wt.% ZIF-90/PVDF dispersion in DMF: a) dynamic viscosity, b) amplitude sweep, and c) frequency sweep curves. The storage *G'* and loss *G''* moduli measured in each run are represented in the same colour for convenience of reading.

II. Scanning Electron Microscopy (SEM)

Fig. S4 shows the cross sections of the neat PVDF as well as the ZIF-90/PVDF MMMs. These lower magnification images show that the thickness of the membrane is ranging from ~40-60 µm. The apparently rough morphology of the cross-sectional surface was a result of fracturing the membranes in liquid nitrogen.

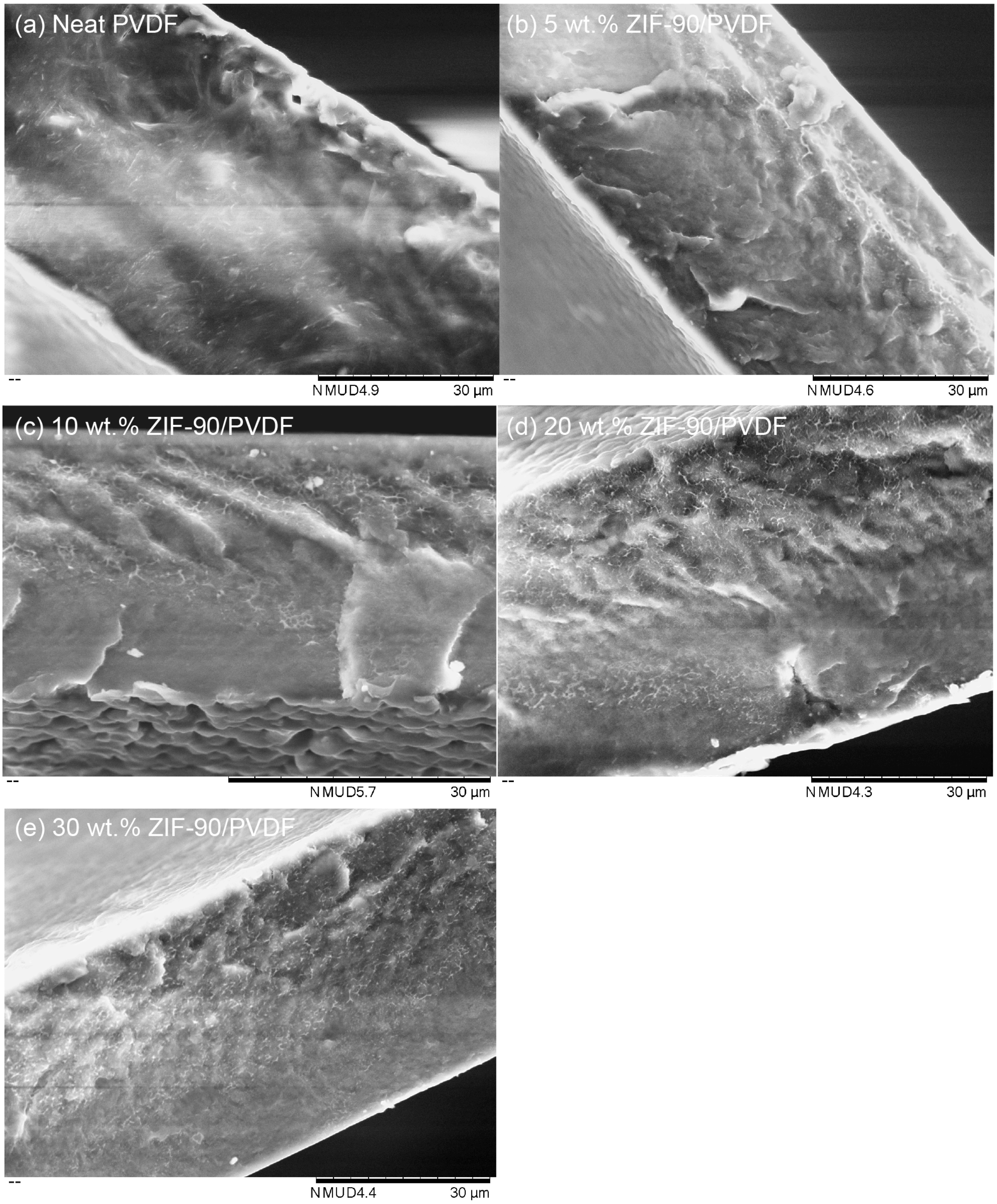

Fig. S4. SEM images of cross sections of the neat PVDF and ZIF-90/PVDF MMMs.

III. Uniaxial Tensile Tests

Fig. S5 shows stress-strain curves obtained for the MMMs using a tensile testing machine at a constant displacement rate of 2 mm min^{-1}. Here we show that it is important to test multiple samples because of the variability in the elongation-to-failure (strain % at fracture).

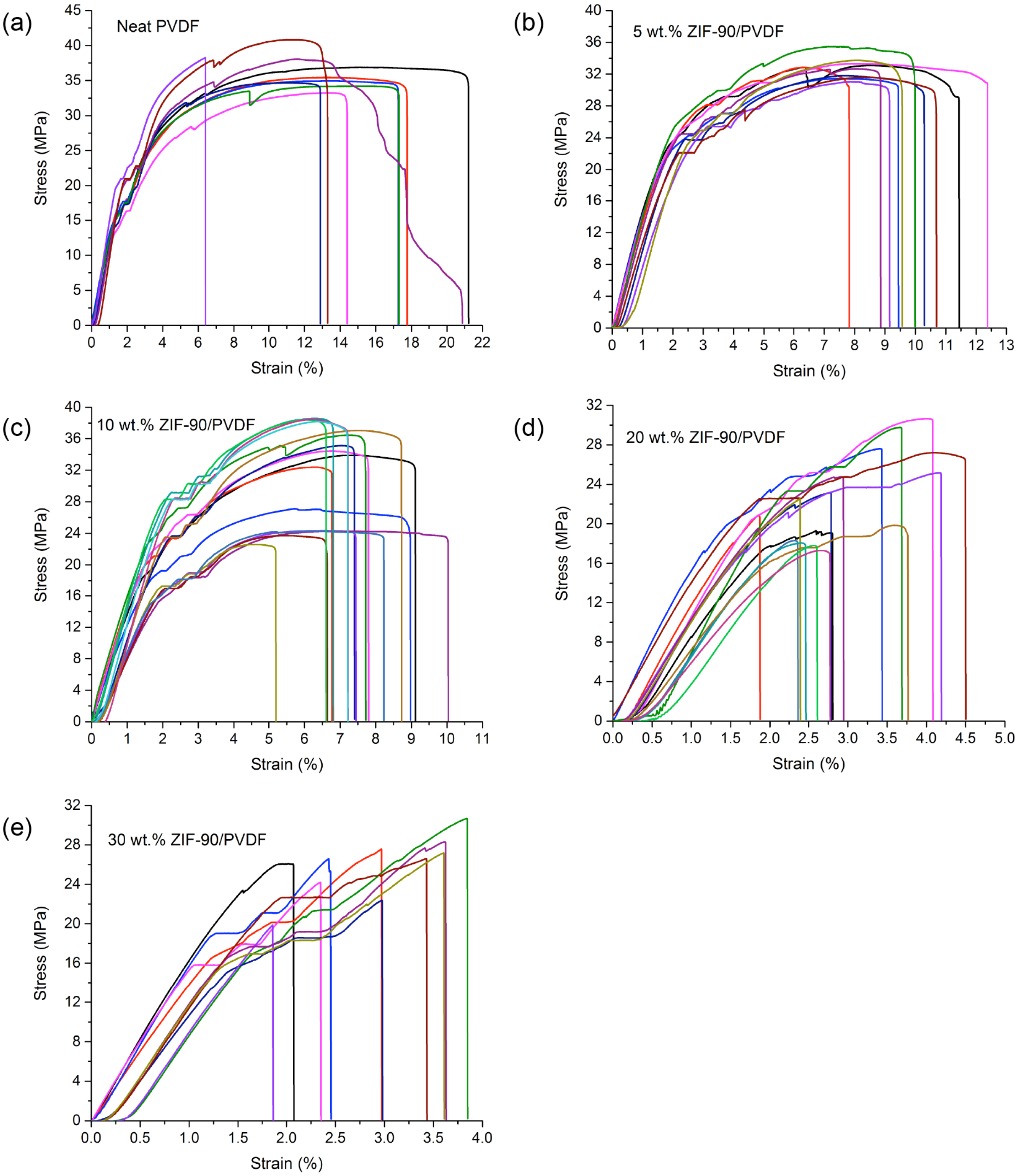

Fig. S5. Stress-strain curves of a) neat PVDF, b) 5 wt.%, c) 10 wt.%, d) 20 wt.%, and e) 30 wt.% ZIF-90/PVDF MMMs.

IV. Nanoindentation

Fig. S6 presents the load-displacement curves obtained in the experiments on nanoindentation of the MMMs' top surface. Fig. S7 shows the averaged indentation modulus and hardness of the MMMs with error bars derived from at least 15 individual indention measurements.

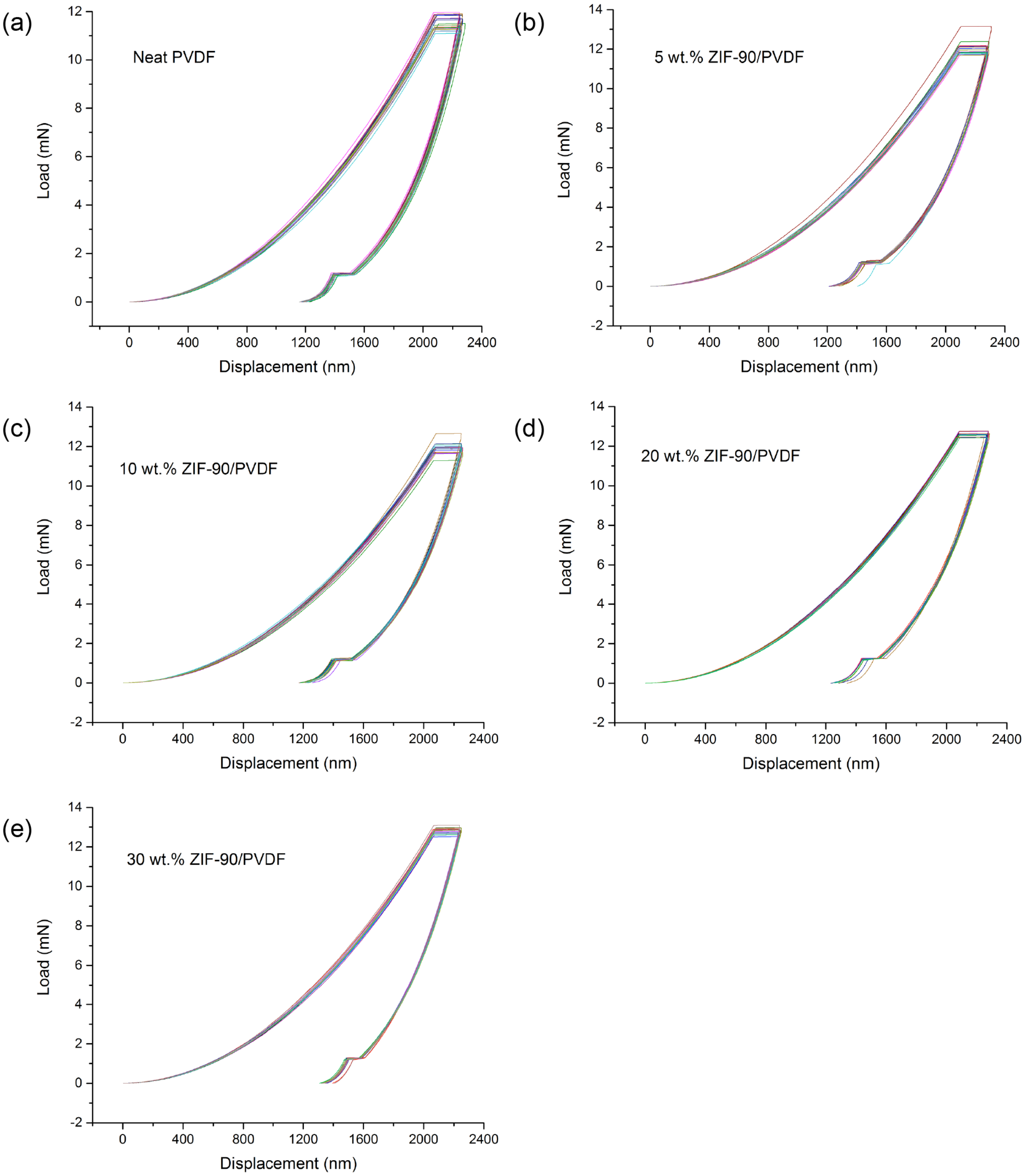

Fig. S6. Load – displacement (P-h) nanoindentation curves of a) neat PVDF and the MMMs: b) 5 wt.%, c) 10 wt.%, d) 20 wt.%, and e) 30 wt.% ZIF-90/PVDF.

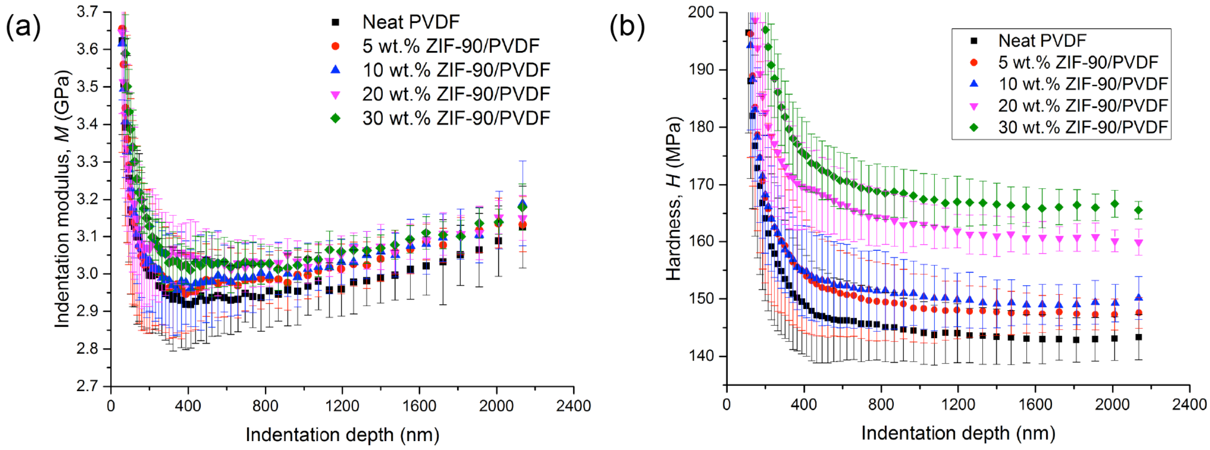

Fig. S7. Indentation modulus a) and hardness b) of the ZIF-90/PVDF membranes. Values below a depth of 200 nm are due to indenter tip calibration artefacts, therefore averaged values reported in Fig.4 of the manuscript were derived from the depths of between 200-2000 nm only.

V. Dynamic Mechanical Analysis (DMA)

DMA measurements were performed under the tensile mode for specimens with a gauge length of 12.5 mm and a width of 5 mm. The storage modulus (E'), loss modulus (E''), and loss tangent (tan δ) at 5 Hz are presented in Fig. S8-S10 respectively. Multiple specimens (~5 of each wt%) were tested to ensure sufficient reproducibility, thus the curves formed "bands" showing that there was some material variability even in the neat PVDF matrix.

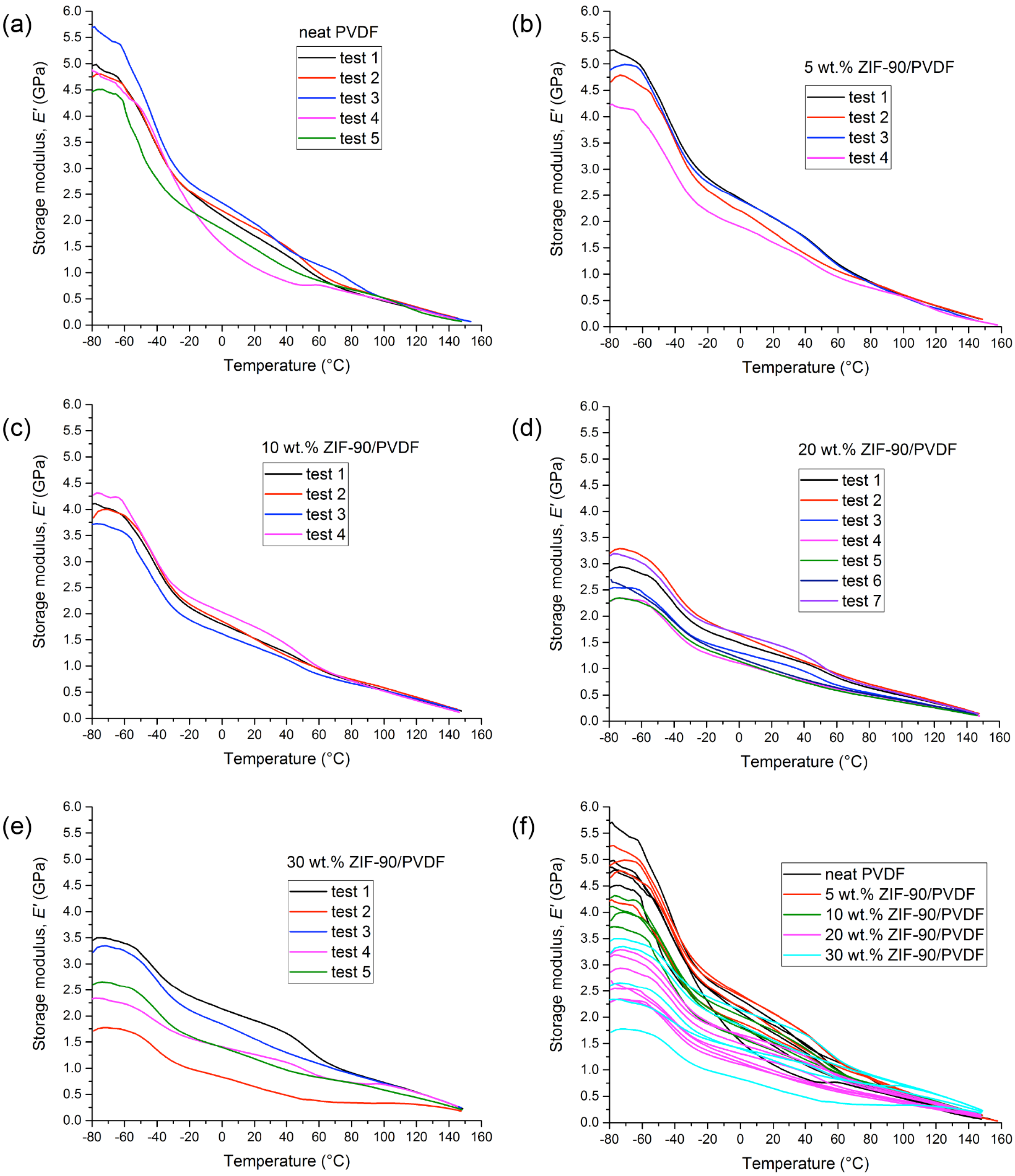

Fig. S8. DMA storage modulus E' curves, forming bands for each of the ZIF-90 wt.% loadings. The legends show the number of tests.

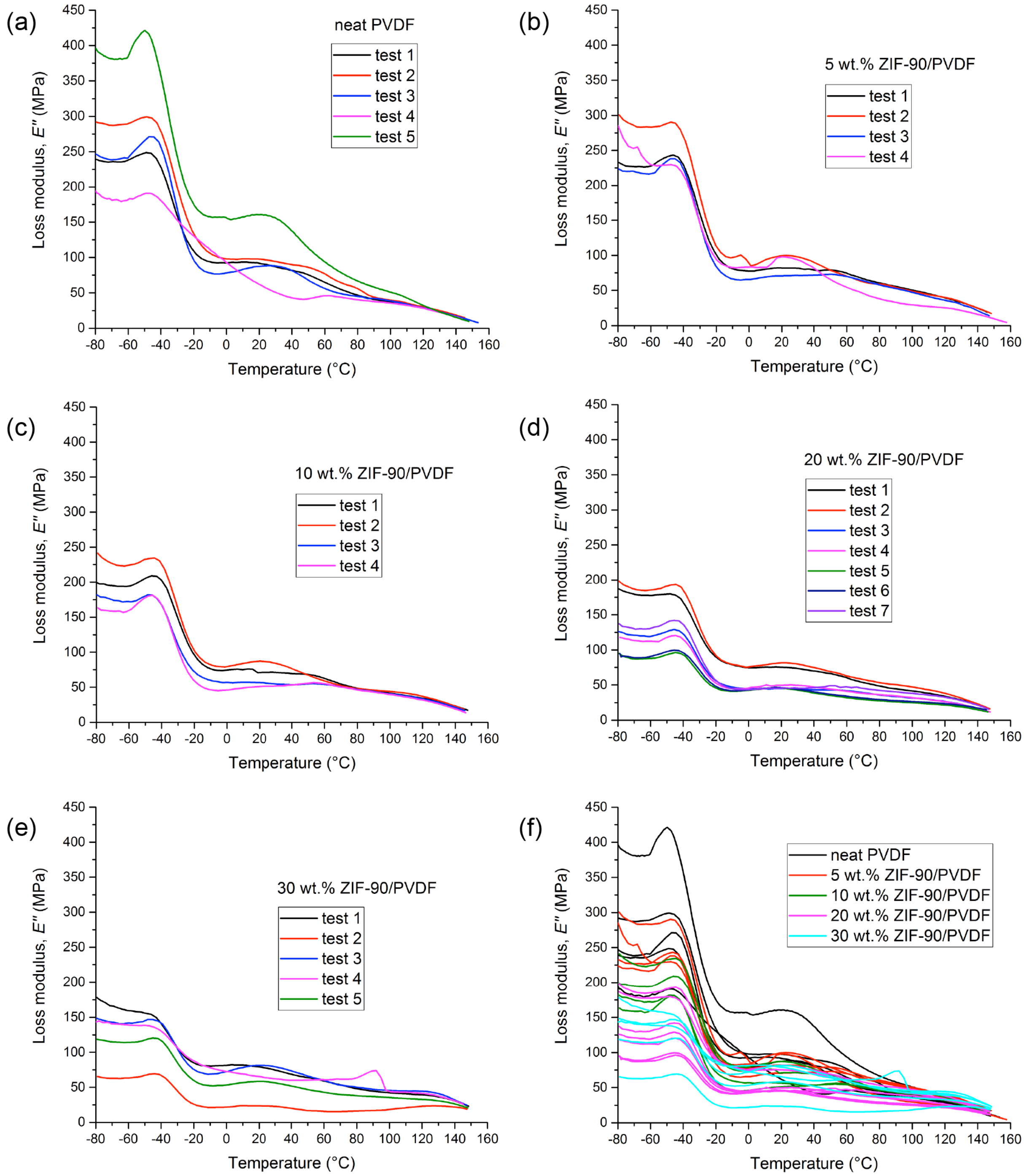

Fig. S9. DMA loss modulus *E"* curves, forming bands for each of the ZIF-90 wt.% loadings. The legends show the number of tests. The glass transition temperature of PVDF is at around -40°C.

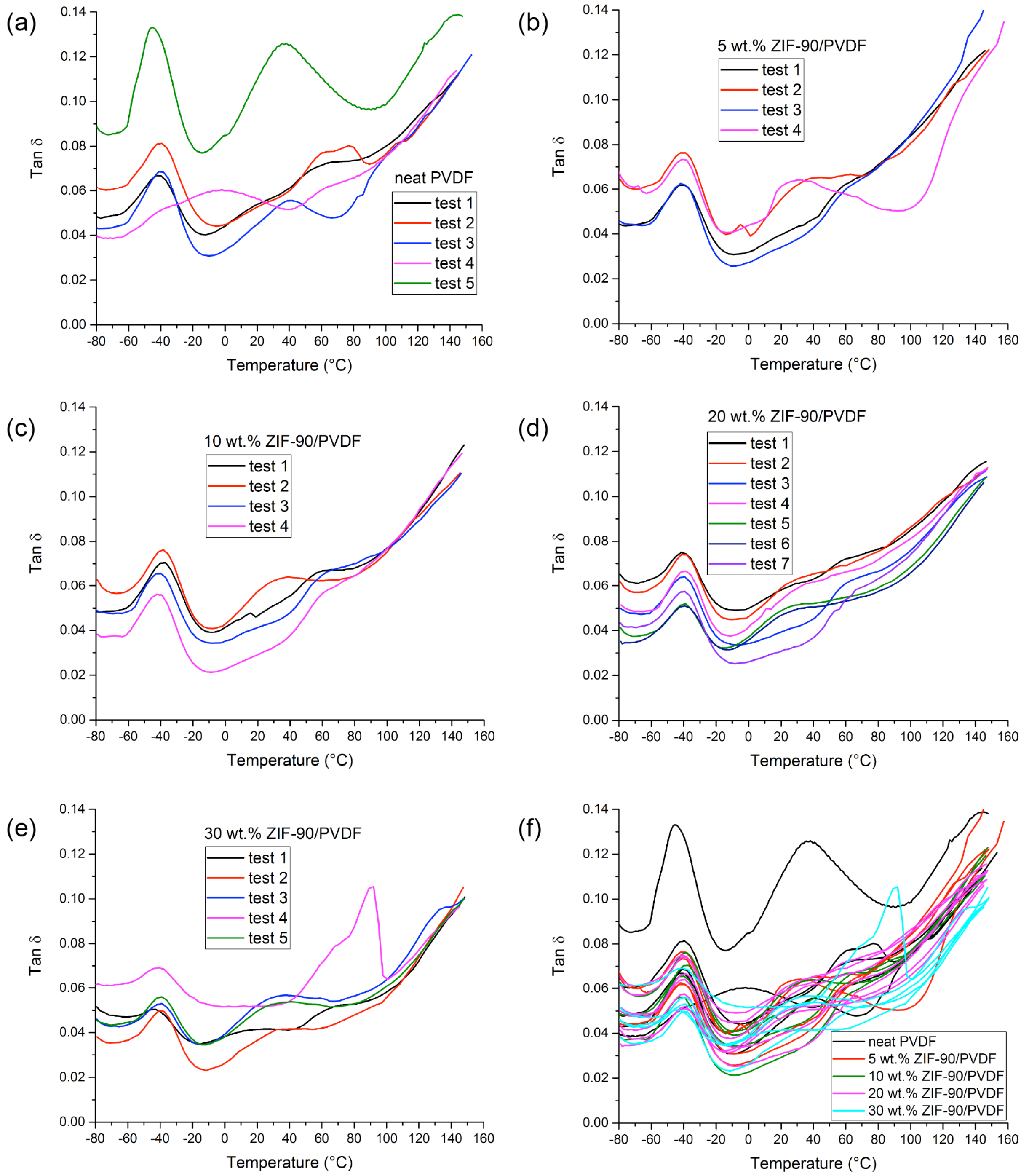

Fig. S10. Loss tangent curves, where Tan (δ) = *E*''/*E*'. The legends show the number of tests of each wt.% loading. The glass transition temperature of PVDF is at around -40°C.